The Astronomical Journal, 130:635–642, 2005 August


# THE OPEN CLUSTER NGC 6520 AND THE NEARBY DARK MOLECULAR CLOUD BARNARD 86

Giovanni Carraro,[1,2] René A. Méndez, Jorge May, and Diego Mardones
Departamento de Astronomía, Universidad de Chile, Casilla 36-D, Santiago, Chile; gcarraro@das.uchile.cl, rmendez@das.uchile.cl, jorge@das.uchile.cl, mardones@das.uchile.cl
*Received 2005 January 7; accepted 2005 April 19*

## ABSTRACT

Wide-field *BVI* photometry and $^{12}$CO ($1 \rightarrow 0$) observations are presented in the region of the open cluster NGC 6520 and the dark molecular cloud Barnard 86. From the analysis of the optical data we find that the cluster is rather compact, with a radius of $1.'0 \pm 0.'5$, smaller than previous estimates. The cluster age is $150 \pm 50$ Myr, and the reddening $E_{B-V} = 0.42 \pm 0.10$. The distance from the Sun is estimated to be $1900 \pm 100$ pc, which is larger than previous estimates. We finally derive basic properties of the dark nebula Barnard 86 on the assumption that it lies at the same distance as the cluster.

*Key words:* ISM: clouds — ISM: individual (Barnard 86) — open clusters and associations: general — open clusters and associations: individual (NGC 6520)

## 1. INTRODUCTION

NGC 6520 (C1800-279; $\alpha = 18^{\rm h}03^{\rm m}24^{\rm s}$, $\delta = -27^\circ 54' 0''$, $l = 2.^\circ 87$, $b = -2.^\circ 85$ [J2000.0]) is a compact moderate-age open cluster located in the Sagittarius constellation only 4° eastward of the Galactic center direction. The region is very crowded (see Fig. 1) and also harbors the dark molecular cloud Barnard 86 ($l = 2.^\circ 85$, $b = -2.^\circ 75$; Barnard 1927), a few arcminutes westward of the cluster. The cloud is a very prominent feature, but other dust lanes are present across the field. In particular, the feature extends toward the cluster, and it is readily visible southward. Moreover, by inspecting more closely Figure 1, or sky maps, one has the clear impression that the dark nebula encompasses the whole cluster. This implies that across the region we expect the reddening to vary significantly, although within the small cluster radius variable reddening should not be a real issue. It seems quite natural to look for a possible relationship between the cluster and the cloud, because of their proximity. Their mutual relationship could in fact turn out to be quite important for our understanding of the timing and outcomes of star cluster formation processes. To address this issue, we obtained wide-field optical photometry in the *BVI* filters and $^{12}$CO ($1 \rightarrow 0$) data, which are presented and discussed in this paper. The aim is to derive estimates of the cluster and cloud distances from the Sun, which is the basic step to clarifying their possible relationship.

The paper is organized as follows. Section 2 illustrates the data acquisition details and the data reduction procedures. Section 3 is dedicated to the analysis of the optical data and the derivation of NGC 6520's fundamental parameters. Section 4 deals with the determination of Barnard 86's physical parameters, while § 5 highlights the paper results and proposes future lines of investigation.

## 2. OBSERVATIONS AND DATA REDUCTION

This section illustrates the data acquisition and the employed reduction techniques.

### 2.1. *Optical Photometry*

*BVI* photometry of two overlapping fields in the region of NGC 6520 and Barnard 86 was taken at the Cerro Tololo Inter-American Observatory (CTIO) 0.90 m telescope on the nights of 1999 June 24 and 25. The pixel scale of the $2048 \times 2046$ Tek2k No. 3 CCD is $0.''396$, allowing observation of a field of $13.'5 \times 13.'5$ in the sky. The total covered area amounts to $20.'0 \times 13.'5$. The two nights were photometric with an average seeing of $1.''3$. We took several short (5 s), medium (300 s), and long (600 s) exposures in all the filters to avoid saturation of the brightest stars. The data have been reduced with the IRAF[3] packages CCDRED, DAOPHOT, ALLSTAR, and PHOTCAL using the point-spread function method (Stetson 1987). Calibration was secured through the observation of Landolt (1992) standard fields G26, PG 1047, PG 1323, PG 1633, PG 1657, SA 110, and SA 112 for a grand total of 90 standard stars. The calibration equations turned out to be of the form

$$b = B + (2.778 \pm 0.007) + (0.25 \pm 0.01)X - (0.092 \pm 0.007)(B - V)$$

$$v = V + (2.595 \pm 0.008) + (0.16 \pm 0.01)X + (0.030 \pm 0.007)(B - V)$$

$$v = V + (2.595 \pm 0.008) + (0.16 \pm 0.01)X + (0.026 \pm 0.006)(V - I)$$

$$i = I + (3.554 \pm 0.005) + (0.08 \pm 0.01)X + (0.029 \pm 0.004)(V - I),$$

and the final rms of the calibration turned out to be 0.03 for all the passbands. Photometric errors were estimated following Patat & Carraro (2001). It turns out that stars brighter than $V \approx 20$ mag have internal (ALLSTAR output) photometric errors lower than 0.15 mag in magnitude and lower than 0.21 mag in color. The final photometric data (coordinates and *B*, *V*, and *I* magnitudes and errors) consisting of 50,000 stars will be made available in electronic form at the WEBDA[4] Web site maintained by J.-C. Mermilliod. Finally, we estimated the completeness of our samples in the *V* and *I* filters. The completeness

[1] Astronomy Department, Yale University, New Haven, CT 06511.
[2] On leave from Dipartimento di Astronomia, Università di Padova, Vicolo Osservatorio 5, I-35122 Padua, Italy.
[3] IRAF is distributed by the National Optical Astronomy Observatory, which is operated by the Association of Universities for Research in Astronomy, Inc., under cooperative agreement with the National Science Foundation.
[4] See http://obswww.unige.ch/webda/navigation.html.

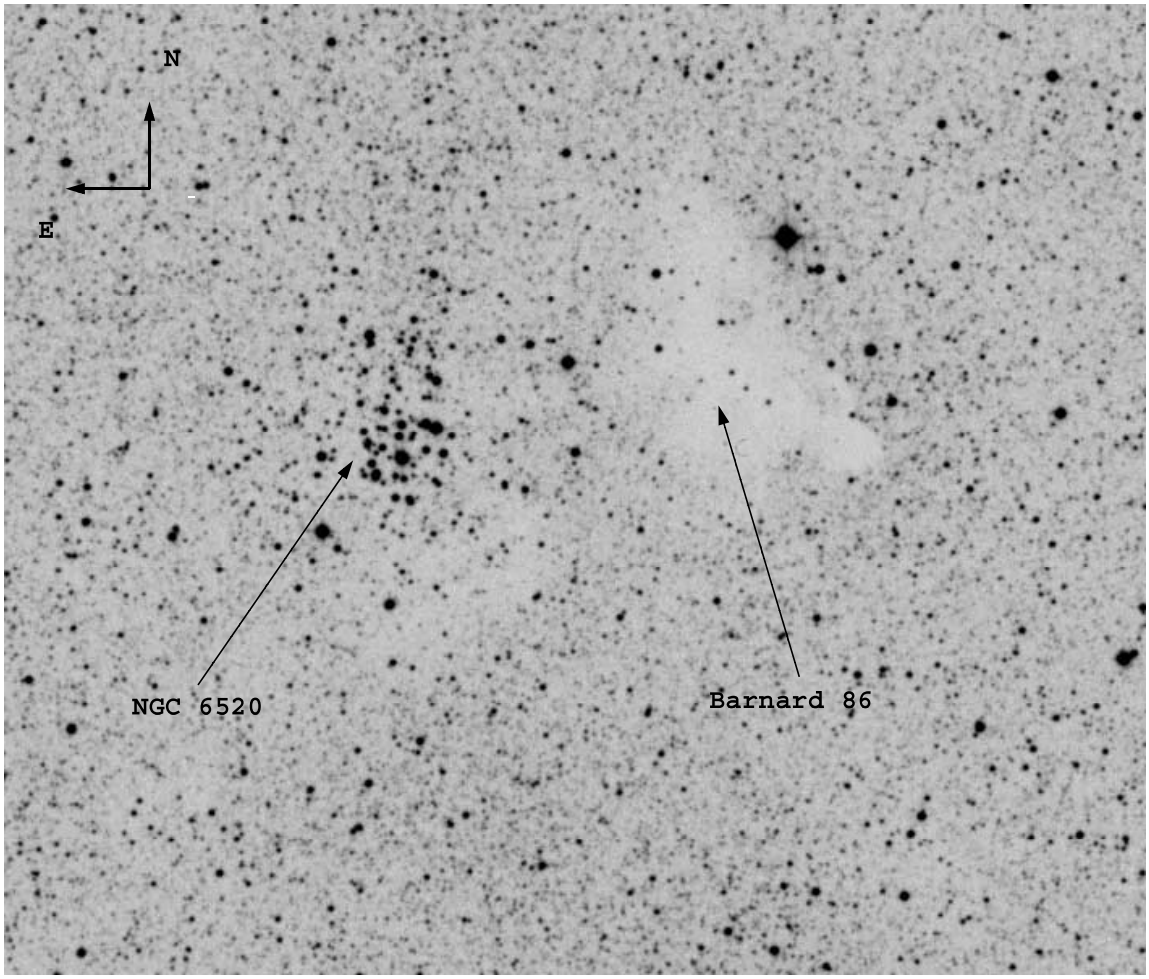


FIG. 1.—DSS map of the observed field in the direction of NGC 6520 and Barnard 86. The size of the field is $20' \times 13'.5$.

corrections were determined by standard artificial-star experiments on our data (see Carraro et al. 2005). Basically, we ran the ADDSTAR task several times, adding 15% of the number of detected stars, counting the number of stars with the ALLSTAR task after performing all the steps and using the same parameters as for the original images. In each run, a new set of artificial stars, following a similar magnitude distribution, was added at random positions. A comparison between the amount of added and detected stars, also taking into account that not all the stars are detected in both the $V$ and $I$ filters, yields a completeness level of 100% down to $V = 16$ and larger than 60% down to $V = 20$. At fainter magnitudes, the completeness level falls below 50%, and therefore we are considering $V = 20$ as our limiting magnitude for the purpose of deriving the cluster mass (but see also § 3.1).

### 2.2. CO *Observations*

The observations were carried out in 1998 September with the Columbia University–Universidad de Chile Millimeter-Wave Telescope (Cohen 1983; Bronfman et al. 1988) located at CTIO. The telescope is a 1.2 m Cassegrain with a beamwidth of $8'.8$ (FWHM) at 115 GHz, the frequency of the CO ($J = 1 \rightarrow 0$) transition. It was equipped with a superheterodyne receiver with a single-sideband noise temperature of 380 K. The first stage of the receiver consisted of a Schottky-barrier diode mixer and a GaAs field-effect transistor amplifier cooled to 77 K by liquid nitrogen.

The spectrometer was a 256 channel filter bank of standard NRAO design. Each filter, 100 kHz wide, provided a velocity resolution of 0.26 km s$^{-1}$ at 115 GHz and a coverage of 66 km s$^{-1}$. The integration time for each position varied between 10 and 12 minutes, depending on source altitude and atmospheric opacity. Spectra were individually intensity-calibrated against a blackbody reference by the standard chopper-wheel method (e.g., Kutner & Ulich 1981 and references therein), yielding a temperature scale $T_a^*$ corrected for atmospheric attenuation, resistive losses, and rearward spillover and scattering. A sampling interval of $3'.75$ ($0^\circ.0625$) was used, almost half of the beamwidth, to optimize the angular resolution of the instrument. Position switching was used for all the observations, with equal amounts of time spent on the source and on the reference positions. This radio telescope has a main-beam efficiency of 0.82 (Bronfman et al. 1988).

## 3. STUDY OF THE OPEN CLUSTER NGC 6520

In this section we use the optical data to derive NGC 6520's basic parameters, namely, radius, reddening, distance, and age, by means of star counts and isochrone fitting in the color-magnitude diagrams (CMDs). The cluster was already studied in the past. The most recent study is by Kjeldsen & Frandsen (1991), who obtained CCD *UBV* photometry of about 300 stars in a $4'.0 \times 2'.6$ area and found that NGC 6520 is a 190 Myr old cluster located 1.60 kpc from the Sun with a reddening $E_{B-V} = 0.43$. These results basically agree with previous investigation (Svolopoulos 1966). We observed 50,000 stars down to $V \approx 21$. We compared our photometry with that of Kjeldsen & Frandsen (1991) and generally found a very good agreement at the level of

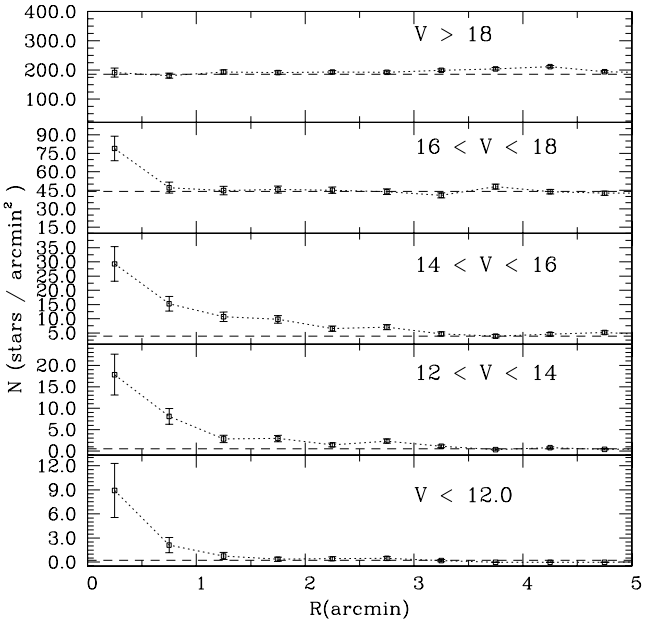


FIG. 2.—Star counts as a function of radius from the adopted cluster center for various magnitude intervals. The dashed line in each panel indicates the mean density level of the surrounding Galactic disk field in that magnitude level.

0.01 mag, except for the brightest stars ($V \leq 11.4$), where our stars are brighter than those of Kjeldsen & Frandsen (1991) by 0.2–0.3 mag. We believe that this is due to saturation problems in the Kjeldsen & Frandsen (1991) photometry.

### 3.1. *Star Counts and Cluster Size*

The aim of this section is to obtain the surface density distribution of NGC 6520 and derive the cluster size in the magnitude space by means of star counts. The cluster radius is indeed one of the most important cluster parameters, useful (together with cluster mass) for a determination of cluster dynamical parameters. Star counts allow us to determine statistical properties of clusters (as visible star condensations) with respect to the surrounding stellar background. As shown in Figure 1, NGC 6520 appears as a concentration of bright stars in a region of about $1'$–$2'$. In order to derive the radial stellar surface density we first look for the highest peak in the stellar density to find out the cluster center. The adopted center is placed at $\alpha = 18^{\rm h}03^{\rm m}24\overset{\rm s}{.}0$, $\delta = -27^\circ 53' 18\overset{''}{.}0$, as given by Dias et al. (2002). Then the radial density profile is constructed by performing star counts inside increasing concentric annuli $0\overset{'}{.}5$ wide around the cluster center and then dividing by their respective surfaces. This is done as a function of apparent magnitude and compared with the mean density of the surrounding Galactic field in the same brightness interval. The contribution of the field has been estimated through star counts in the region outside $6'$ from the cluster center. Poisson standard deviations have also been computed and

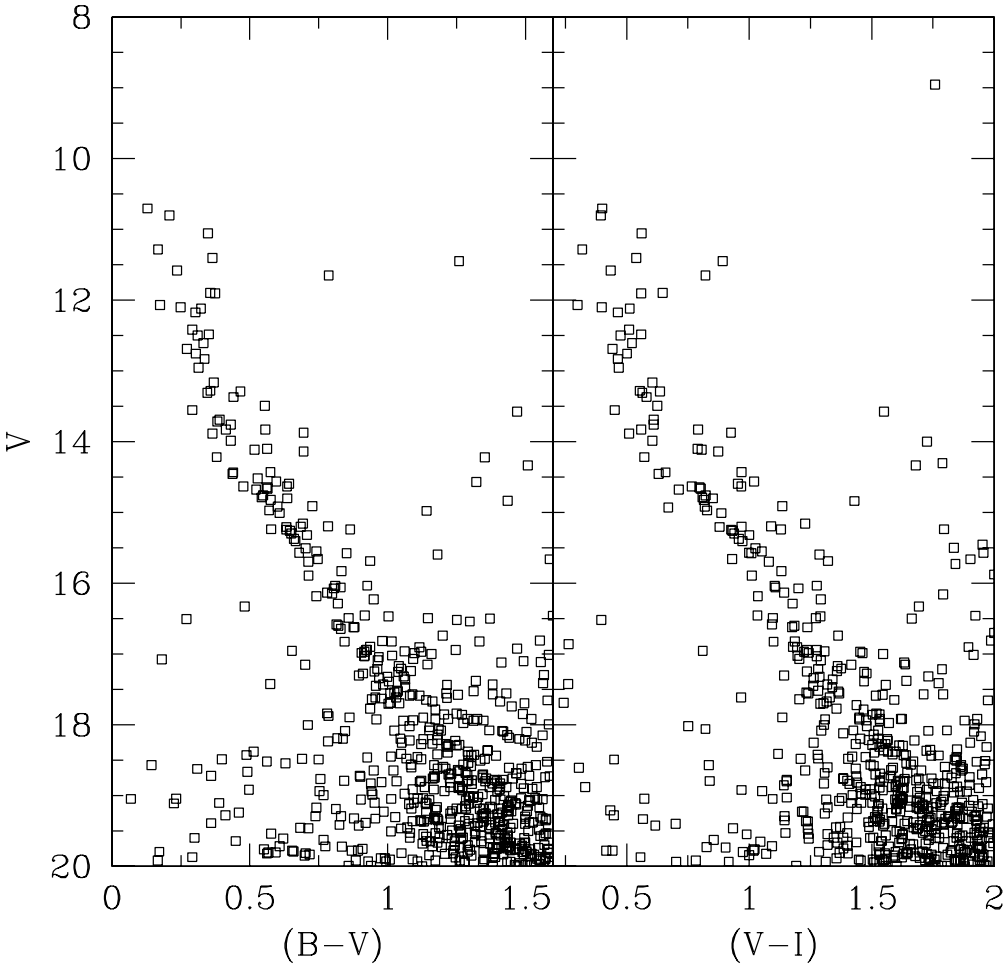


FIG. 3.—CMDs for the stars in the field of NGC 6520. *Left*: $V$ vs. $(B - V)$. *Right*: $V$ vs. $(V - I)$.

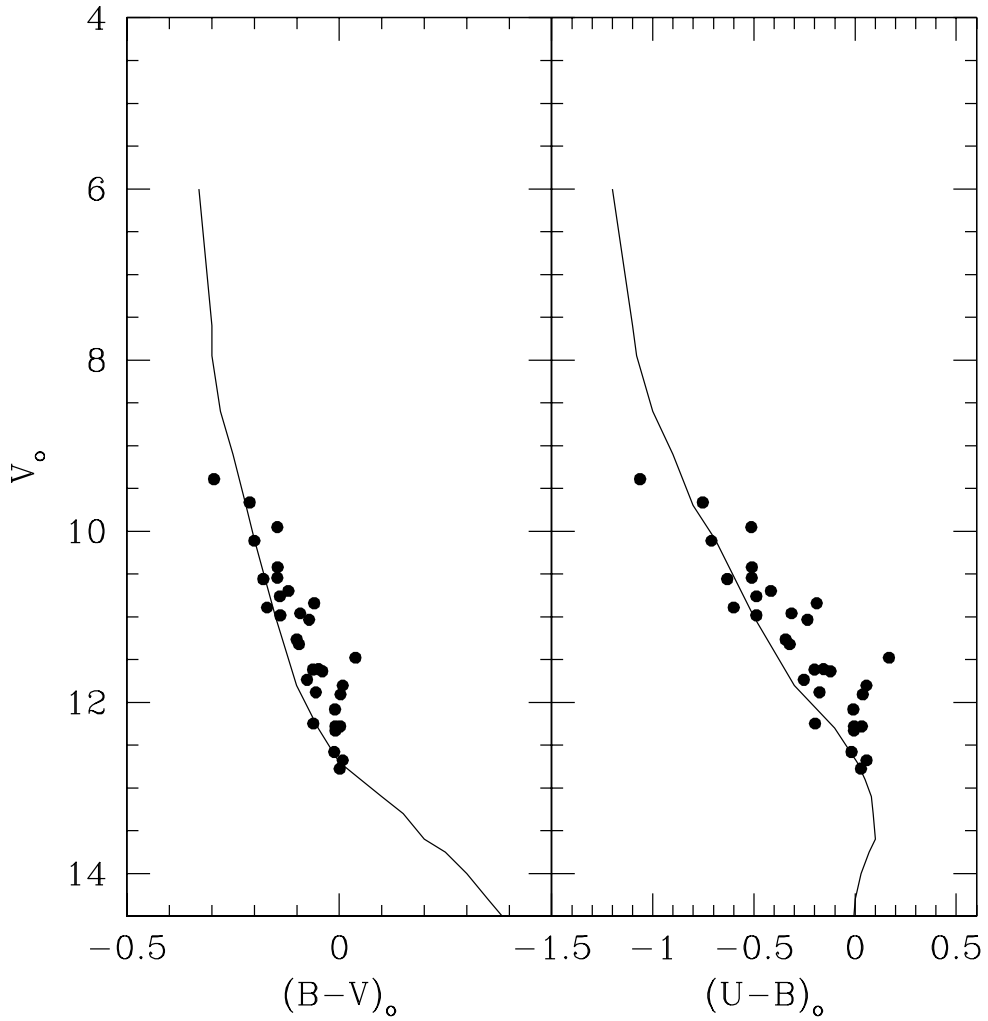


FIG. 4.—Reddening-corrected CMDs from *UBV* photometry of Kjeldsen & Frandsen (1991). Superposed in both panels is the empirical ZAMS from Schmidt-Kaler (1982). See text for more details.

normalized to the area of each ring as a function of magnitude, both for the cluster and for the field. The result is shown in Figure 2, where one readily sees that NGC 6520 significantly emerges from the mean field above $V \approx 18$. At fainter magnitudes the cluster gets confused with the Galactic disk population. Based on the radial density profiles in Figure 1, we find that stars brighter than $V = 18$ provide a cluster radius smaller than $2'$. We adopt as a final estimate of the radius the value $1.'0 \pm 0.'5$. This is somewhat smaller than the estimate of $2.'5$ reported by Dias et al. (2002), which was simply based on visual inspection. We adopt this value of the cluster radius throughout this work. We stress, however, that this radius is not the limiting radius of the cluster but the distance from the cluster center at which the cluster population starts to be confused with the field population.

### 3.2. *Analysis of the CMDs*

The *BVI* photometry allows us to build up CMDs in the $(V, B - V)$ and $(V, V - I)$ planes. They are shown in Figure 3, in which we consider only the stars located within $1'$ of the cluster center. The main sequence (MS) extends from $V = 11$ to 20, although at $V = 18$ the contamination by foreground stars starts to be significant. The MS has a width of about 0.2–0.3 mag, a bit larger than expected from simply photometric errors (see § 2). There might be some differential reddening across the cluster area, but we believe it is not very important. Unfortunately, we do not have $U$ photometry, but from the two-color $(U - B)$ versus $(B - V)$ diagram by Kjeldsen & Frandsen (1991), one readily sees that the amount of differential reddening does not exceed 0.10 mag. Therefore, differential reddening does not play an important role in a cluster that compact, and the MS width might be the result of the combination of the two effects plus some probable interlopers and/or binary stars. The detailed shape of the turnoff (TO) region is much better defined than in Kjeldsen & Frandsen (1991) and deserves more attention, since the scatter of stars there is much larger than in the MS. The MS seems to stop at $V = 12.5$ and $(B - V) = 0.25$ [$(V - I) = 0.35$], and the brighter stars clearly are in the act of leaving it, since they lie redward of the MS. We are keen to believe that the few stars above the TO brighter than $V = 12$ are field stars or blue stragglers, which are frequent in open star clusters. The global shape of the CMD is that of an open cluster of moderate age, such as NGC 6204 (Carraro & Munari 2004) or NGC 2287 (Harris et al. 1993).

### 3.3. *NGC 6520 Basic Parameters*

The fundamental parameters of NGC 6520 have already been derived in the past. Both Svolopoulos (1966) and Kjeldsen & Frandsen (1991) agree that the cluster possesses a heliocentric distance of about 1600 pc and a reddening $E_{B-V} = 0.42$. As for the age, there are some contradictory findings in the literature.

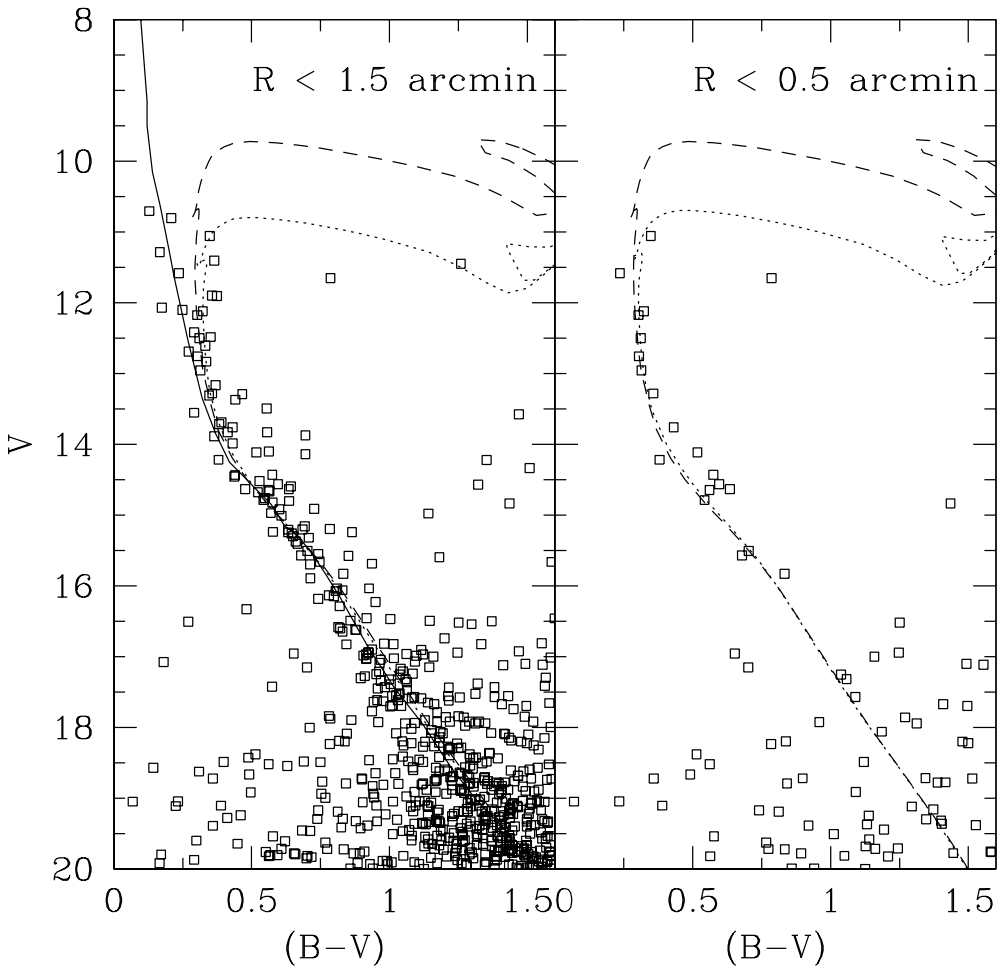


FIG. 5.—CMDs of NGC 6520 as a function of radius. Superposed is the empirical ZAMS from Schmidt-Kaler (1982; *solid line*) and two solar abundance isochrones for the ages of 100 (*dashed lines*) and 200 (*dotted lines*) million years. In the right panel only stars within 0.′5 of the cluster center are considered in order to minimize the effect of field star contamination in the age derivation.

In fact, while Svolopoulos (1966) reports an age of 800 Myr, Kjeldsen & Frandsen (1991) suggest a much younger age of 190 Myr. This is clearly due to the scatter in the upper part of the MS, which makes it difficult to recognize the TO point. Before analysis of our data we made use of the Kjeldsen & Frandsen (1991) *UBV* photometry to select photometric members based on the *Q* method (Carraro 2002), and from the reddening-corrected CMDs (see Fig. 4) we derived an absolute distance modulus $(m - M)_0 = 11.40$ by fitting an empirical zero-age main sequence (ZAMS) from Schmidt-Kaler (1982). Although the sequence is vertical and there might be problems with the magnitudes of the brightest stars (see § 3), the fit is quite good in both CMDs and provides a distance of $1900 \pm 100$ pc.

In addition, we derive NGC 6520's fundamental parameters by directly comparing the CMD with theoretical isochrones from the Padua group (Girardi et al. 2000). The results of the fit are presented in Figures 5 and 6. In Figure 5 (*left*) we plot the $(V, B - V)$ CMD for all the stars within 1.′5 of the cluster center. Superposed is a ZAMS from Schmidt-Kaler (1982; *solid line*) shifted by $(m - M)_V = 12.75 \pm 0.10$ and $E_{B-V} = 0.42 \pm 0.10$ (error by eye), which fits very well the bulk of the cluster MS. Together with the ZAMS, we superposed two solar-metallicity isochrones for the ages of 100 (*dashed line*) and 200 (*dotted line*) million years from Girardi et al. (2000) shifted by $(m - M)_V = 12.65$ and $E_{B-V} = 0.40$ and $(m - M)_V = 12.75$ and $E_{B-V} = 0.42$, respectively. This fit provides an estimate of the cluster distance from the Sun, which turns out to be 1950 pc. This estimate is about 20% larger than the previous one by Kjeldsen & Frandsen (1991), and we believe that this is due to the saturation of bright stars in Kjeldsen & Frandsen (1991), which prevented clear definition of the upper part of the MS. However, on the basis of this CMD, one cannot exclude a younger age, as a result of the presence of several bright stars along the ZAMS. To better understand the nature of these stars, we isolate in Figure 5 (*right*) the stars within 0.′5 of the cluster center in order to minimize the effect of field star contamination. The fit is still very good and confirms previous findings about the distance and reddening, suggesting that the bright stars are just interlopers.

As for the age, a close scrutiny of the TO region clearly favors an age around 200 million years. This is confirmed by the absolute magnitudes and colors of the brightest photometric members. With a TO located at $V \approx 12.5-13$, we expect that unevolved stars still in the MS have $M_V$ in the range $-0.25$ to 0.25 and therefore a spectral type around B5–B8, which implies an age around 150 million years (Girardi et al. 2000).

Finally, in Figure 6 we achieve the same fit both in the $(V, B - V)$ diagram (*left*) and in the $(V, V - I)$ diagram (*right*). Here we again provide a reasonable fit to the data for the same distance modulus and a reddening $E_{V-I} = 0.55$. The ratio $E_{V-I}/E_{B-V}$ turns out to be 1.30, not far from the widely used 1.24 value from

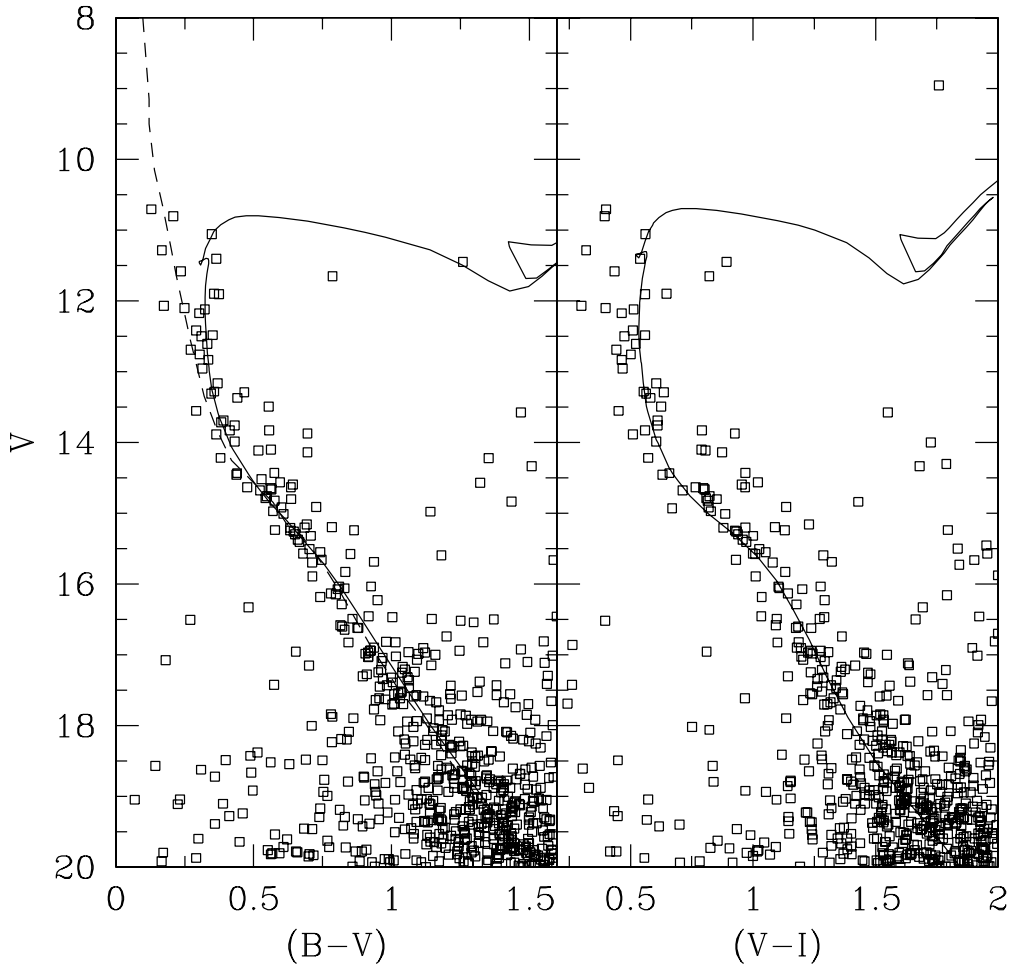


FIG. 6.—CMDs of Fig. 3. Superposed in the left panel is a Schmidt-Kaler (1982) ZAMS (*dashed line*) and a solar-metallicity isochrone (*solid line*) for the age of 200 Myr shifted by $E_{B-V} = 0.42$ and $(m - M)_V = 12.75$. In the right panel the same isochrone is shifted by $E_{V-I} = 0.55$ and $(m - M)_V = 12.75$.

Dean et al. (1978). In conclusion, we estimate the age of NGC 6520 to be 150 ± 50 Myr and provide a distance of about 1900 ± 100 pc, 20% larger than previous estimates.

### 3.4. *NGC 6520 Mass*

In order to derive the cluster mass we first derived the cluster luminosity function and mass function (MF) in the same way as in Carraro et al. (2005). Briefly, we considered only the stars within 1.′5 of the cluster nominal center and brighter than $V = 18$ (see § 3.1), and we statistically derived the cluster population by subtracting the field population from a same-area region outside 6′ from the cluster nominal center. The subtraction was made bin by bin, with a bin size of 0.5 mag, and each bin population was corrected for the corresponding incompleteness. The MF turned out to be a power law with slope $\alpha = 2.4 \pm 0.3$ and therefore compatible with the standard Salpeter (1955) MF. By integrating the MF over the $V$ magnitude range 11–18, we estimated that the cluster mass is $364 \pm 54\ M_{\odot}$.

## 4. THE DARK CLOUD BARNARD 86

In this section we derive the physical parameters of the molecular cloud associated with Barnard 86 obtained from a Gaussian fit to its composite spectrum, i.e., the sum of all spectra across the cloud's projected surface. The quality of the spectra is shown in Figure 7, together with the best Gaussian fit. The figure shows the average of the two brightest CO (1 → 0) spectra. The cloud is clearly detected in at least nine positions within a 30 position map. The rms noise of the spectrum shown is 0.15 K. The intensity scale is in antenna temperature, uncorrected by the main-beam efficiency. This is a 9 $\sigma$ detection at the peak, or a 15 $\sigma$ detection of the integrated intensity. The only effect of combining the central two spectra is to reduce the noise by a factor of 1.41, but the detection is strong in both spectra.

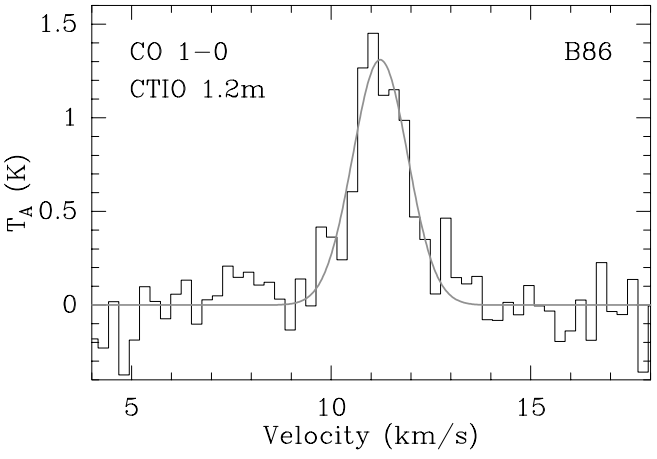


FIG. 7.—Average of the two brightest CO (1 → 0) spectra in the region of Barnard 86. The superposed line is the Gaussian fit.

### 4.1. *Cloud Distance*

We derive the cloud properties by assuming that the nebula lies at the same distance as the cluster NGC 6520. This is naturally a crude assumption, which is mainly motivated by the appearance of Figure 1. The center of the dark nebula lies 6′ from the cluster center, but the two objects do not appear clearly detached. The whole cluster seems to be surrounded by some nebulosity, which gets denser in the southern regions and seems to form a bridge with the main body of the cloud northwest of the cluster. This is also confirmed by the appearance of the whole region in the Southern H$\alpha$ Sky Survey Atlas (Gaustad et al. 2001), in which one can clearly see that the nebula embraces the cluster. Obviously, this assumption must be verified in some more quantitative way, which is not possible with the present data. The only way we envisaged was to count the number of stars in front of the cloud and compare this number with the number of stars expected to lie within 1, 2, and 3 kpc of the Sun in the direction of the cloud, as derived from a Galactic model (Mendez & van Altena 1996; Mendez & Guzman 1998). From our photometry we can count in front of the dark cloud 15 stars in the magnitude range $10 \leq V \leq 19$. In the same magnitude range, the Galactic model predicts 3,046, 17,138, and 41,360 stars deg$^{-2}$ within 1, 2, and 3 kpc of the Sun, respectively. By assuming an area of the dark cloud of 4 arcmin$^2$, we expect from the model about 3.5, 19, and 46 stars in the same magnitude range in front of the nebula. Although model-dependent, this result brings some support to our assumption of common distance for the cluster and the dark cloud.

### 4.2. *Results*

The peak of the CO emission turns out to be located at $l = 2\overset{\circ}{.}875$, $b = -2\overset{\circ}{.}8125$. The radial velocity $V_{\rm LSR}$ and the line width $\Delta V_{\rm obs}$ turn out to be $11.28 \pm 0.25$ and $2.07 \pm 0.25$ km s$^{-1}$ and correspond to the peak and the FWHM of the Gaussian fit of the composite spectrum, respectively. The value of the velocity, by the way, is in nice agreement with the 11.6 km s$^{-1}$ estimate by Clemens & Barvainis (1988). Unfortunately, it is not possible to estimate the distance of the cloud from its radial velocity by means of the Milky Way rotation curve because of the particular cloud position, located in the direction of the Galactic center. Adopting the 2 kpc distance, we estimate an effective radius of $5.36 \pm 0.56$ pc. We define the effective radius of the cloud as $(A/\pi)^{1/2}$, where $A$ is the actual projected area obtained from the angular extent of the cloud, measured from the spatial maps.

The luminosity of $^{12}$CO, $L_{\rm CO}$, was found to amount to $(5.1 \pm 0.2) \times 10^{-4}$ K km s$^{-1}$ pc$^2$, where $L_{\rm CO}$ is given by

$$L_{\rm CO} = d^2 I_{\rm CO}, \tag{1}$$

where $I_{\rm CO}$ is the $^{12}$CO line intensity integrated over all velocities and lines of sight within the boundaries of the cloud and $d$ is the heliocentric distance of the cloud (2 kpc).

As for the mass, this is computed from the $^{12}$CO luminosity and turns out to be $M_{\rm CO} = 600 \pm 150\ M_\odot$. The value of $M_{\rm CO}$ was estimated directly from its $^{12}$CO luminosity on the empirically based assumption that the integrated CO line intensity is proportional to the column density of $H_2$ along the line of sight (e.g., Bloemen et al. 1986; Hunter et al. 1997). Thus, the masses were computed using the relation

$$M_{\rm CO} = wXL_{\rm CO}, \tag{2}$$

where $w$ is the mean molecular weight per $H_2$ molecule, $X$ is the constant ratio of $H_2$ column density to integrated $^{12}$CO intensity, and $L_{\rm CO}$ is the $^{12}$CO luminosity. A detailed description of this kind of mass calculation can be found in May et al. (1997) and Murphy & May (1991). It is also possible to derive an estimate of the cloud virial mass. The virial mass $M_{\rm VT}$ was derived using the relation

$$M_{\rm VT} = 126 r_c (\Delta V_{\rm obs})^2, \tag{3}$$

where $M_{\rm VT}$ is in solar mass, $r_c$ is the effective radius of the cloud in parsecs, and $\Delta V_{\rm obs}$ is the half-power full width of the cloud's composite spectrum in kilometers per second. This equation assumes that (1) the cloud is in virial equilibrium; (2) the cloud is spherical with an $r^{-2}$ density distribution, where $r$ is the distance from its center; and (3) the observed $^{12}$CO line width of the cloud is an accurate measure of the net velocity dispersion of its internal mass distribution, which is believed to be clumpy on many scales. Under these assumptions, the mass turns out to be $M_{\rm VT} = 3000\ M_\odot$. Because of the large discrepancy between $M_{\rm CO}$ and $M_{\rm VT}$, we can conclude that this molecular cloud is not in virial equilibrium, and therefore its mass is about 600 $M_\odot$.

## 5. CONCLUSIONS

In this paper we have presented deep CCD *BVI* photometry and $^{12}$CO ($1 \rightarrow 0$) observations in the region of the open cluster NGC 6520 and the dark molecular cloud Barnard 86. We provided updated estimates of the cluster parameters, suggesting that the heliocentric distance is $1900 \pm 100$ pc and the age is $150 \pm 50$ Myr. We then derived Barnard 86's physical parameters on the assumption that the cloud is at the same distance as the cluster.

As we discussed, this assumption in the present study is only motivated by the particular distribution of the nebulosity in the region of the cloud and the cluster, which seems to support some association of the two objects. In Figure 8 we show a Digitized Sky Survey (DSS) map of the region in which the cluster and the cloud are located, and we superpose the isointensity contour in K km s$^{-1}$. The thick line is the FWHM of the Gaussian fit and clearly crosses the cluster. To us this might mean that the nebulosity close to the cluster is related to Barnard 86, although better resolution spectra are necessary to derive firmer conclusions. We corroborated this hypothesis by comparing the number of stars we can see in front of the cloud with the predictions of a Galactic model, and it turned out that their distance of 2 kpc is quite reasonable.

The age of the cluster ($150 \pm 50$ Myr) seems to be incompatible with this assumption, since the mean lifetime of a molecular cloud does not exceed a few times 10 Myr (Blitz & Shu 1980). This makes the hypothesis of the connection between the cloud and the cluster puzzling.

However, if we accept the common distance hypothesis, the scenario one might envisage is that both NGC 6520 and the dark cloud Barnard 86 share the same origin, the latter being the remains of a star formation process that finished about $150 \times 10^6$ yr ago. In this case, Barnard 86 may be an interesting cloud for studying the possible stability of gas condensation over a full Galactic rotation. In fact, to the best of our knowledge, no other clouds are known to show evidence of a possible relation with an open cluster that old. Clearly, our assumption of the distance must be better constrained, and we propose to derive, for instance, the radial velocity of a few NGC 6520 member stars, which should be compared with the cloud velocity or the IR spectra of some bright stars inside the nebula to measure the properties of the $H_3^+$ line (McCall et al. 2003).

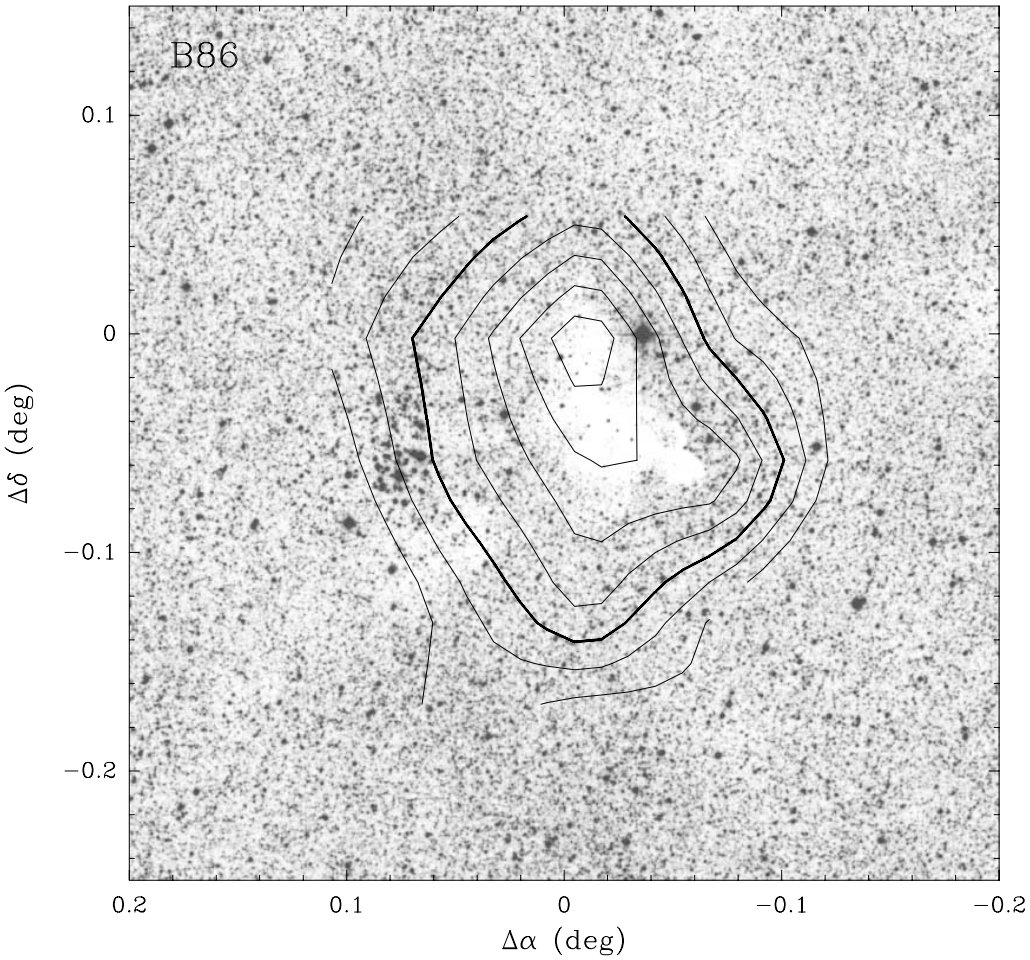


FIG. 8.—DSS map of the region of NGC 6520 and Barnard 86. Superposed are the isointensity contours of the radio observations.

We acknowledge fruitful discussions with S. Casassus and P. Caselli. The work of G. C. is supported by Fundación Andes. R. A. M., J. M., and D. M. acknowledge support from the Chilean Centro de Astrofísica FONDAP 15010003. J. M. acknowledges partial support from FONDECYT through grant 1010431.

REFERENCES

Barnard, E. E. 1927, A Photographic Atlas of Selected Regions of the Milky Way (Washington: Carnegie Inst.)
Blitz, L., & Shu, F. H. 1980, ApJ, 238, 148
Bloemen, J. B. G. M., et al. 1986, A&A, 154, 25
Bronfman, L., Cohen, R. S., Alvarez, H., May, J., & Thaddeus, P. 1988, ApJ, 324, 248
Carraro, G. 2002, MNRAS, 331, 785
Carraro, G., Baume, G., Piotto, G., Mendez, R. A., & Schmidtobreick L. 2005, A&A, 436, 527
Carraro, G., & Munari, U. 2004, MNRAS, 347, 625
Clemens, D. P., & Barvainis, R. 1988, ApJS, 68, 257
Cohen, R. S. 1983, in Surveys of the Southern Galaxy, ed. W. B. Burton & F. P. Israel (Dordrecht: Reidel), 265
Dean, J. F., Warren, P. R., & Cousins, A. W. J. 1978, MNRAS, 183, 569
Dias, W. S., Alessi, B. S., Moitinho, A., & Lepine, J. R. D. 2002, A&A, 389, 871
Gaustad, J. E., McCullough, P. R., Rosing, W., & Van Buren, D. 2001, PASP, 113, 1326
Girardi, L., Bressan, A., Bertelli, G., & Chiosi, C. 2000, A&AS, 141, 371
Harris, G. L. H., FitzGerald, M. P. V., Mehta, S., & Reed, B. C. 1993, AJ, 106, 1533
Hunter, S. D., et al. 1997, ApJ, 481, 205
Kjeldsen, H., & Frandsen, S. 1991, A&AS, 87, 119
Kutner, M. L., & Ulich, N. L. 1981, ApJ, 250, 341
Landolt, A. U. 1992, AJ, 104, 340
May, J., Alvarez, H., & Bronfman, L. 1997, A&A, 327, 325
McCall, B. J., et al. 2003, Nature, 422, 500
Mendez, R. A., & Guzman, R. 1998, A&A, 333, 106
Mendez, R. A., & van Altena, W. F. 1996, AJ, 112, 655
Murphy, D. C., & May, J. 1991, A&A, 247, 202
Patat, F., & Carraro, G. 2001, MNRAS, 325, 1591
Salpeter, E. E. 1955, ApJ, 121, 161
Schmidt-Kaler, T. 1982, in Numerical Data and Functional Relationships in Science and Technology, ed. K. Schaifers & H. H. Voigt (Berlin: Springer), 14
Stetson, P. B. 1987, PASP, 99, 191
Svolopoulos, S. N. 1966, Z. Astrophys., 64, 67